

# Modeling CO<sub>2</sub>-facilitated transport across a diethanolamine liquid membrane

Lihong Bao<sup>a</sup>, Michael C. Trachtenberg<sup>a, b, \*</sup>

<sup>a</sup>Carbozyme Inc., 1 Deer Park Dr., Monmouth Junction, NJ 08852, USA

<sup>b</sup>Sapient's Institute, 1 Deer Park Dr., Monmouth Junction, NJ 08852, USA

Received 6 January 2005; received in revised form 23 May 2005; accepted 26 May 2005

Available online 25 July 2005

## Abstract

We compared experimental and model data for the facilitated transport of CO<sub>2</sub> from a CO<sub>2</sub>-air mixture across an aqueous solution of diethanolamine (DEA) via a hollow fiber, contained liquid membrane (HFCLM) permeator. A two-step carbamate formation model was devised to analyze the data instead of the one-step mechanism used by previous investigators. The effects of DEA concentration, liquid membrane thickness and feed CO<sub>2</sub> concentration were also studied. With a 20% (wt) DEA liquid membrane and feed of 15% CO<sub>2</sub> in CO<sub>2</sub>-air mixture at atmosphere pressure, the permeance reached 1.51E-8 mol/m<sup>2</sup> s Pa with a CO<sub>2</sub>/N<sub>2</sub> selectivity of 115. Model predictions compared well with the experimental results at CO<sub>2</sub> concentrations of industrial importance. Short-term stability of the HFCLM permeator performance was examined. The system was stable during 5-days of testing.

© 2005 Elsevier Ltd. All rights reserved.

**Keywords:** Contained liquid membrane; Gas separation; Mass transfer model; Facilitated transport process

## 1. Introduction

There is a growing concern about the rate of increase in CO<sub>2</sub> released to the atmosphere due to anthropogenic activities because of the possible implications for global climate change. Global fossil-fuel CO<sub>2</sub> emissions reached about 7 × 10<sup>9</sup> tones in year 2000, and the amount is increasing. Thus, it is important to capture and subsequently store CO<sub>2</sub> in a cost effective and safe way.

The best-established method for CO<sub>2</sub> capture is to remove CO<sub>2</sub> by absorption into amine solutions via packed towers, spray towers, or bubble columns (the absorber tower). In a separate tower (the stripper tower), the CO<sub>2</sub> is released from the CO<sub>2</sub>-rich amine solution by heating and the amine is thereby regenerated. This process is known as temperature swing absorption (TSA). However, the

substantial energy requirement for the process forces consideration of more efficient and flexible methods. Two approaches are possible—a change in chemistry or a change in contacting hardware. Here, we focus on the latter as processes employing membrane-based contacting devices have been found promising (Falk-Pedersen et al., 1999). Membrane-based gas absorption techniques operate efficiently and can be adapted easily to the specific demands of an individual plant (Mavroudi et al., 2003).

Kim and Yang (2000) used a microporous PTFE membrane contactor for the separation of CO<sub>2</sub>-N<sub>2</sub> mixtures. The aqueous absorbents used were solutions of monoethanolamine (MEA) and of 2-amino-2-methyl-1-propanol (AMP). Substantial removal of CO<sub>2</sub> was achieved even at very low liquid flow rates. Mavroudi et al. (2003) evaluated the same process for CO<sub>2</sub> removal from flue gas. Using a commercial hollow fiber membrane contactor (Liqui-Gel Extra Flow membrane contactor, Membrana Corp., Charlotte, NC, USA), they demonstrated significant CO<sub>2</sub> removal even when using pure water as absorbent. With the use of an aqueous amine solution (DEA) the CO<sub>2</sub>

\* Corresponding author. Carbozyme Inc., Research and Development Department, 1 Deer Park Dr., Ste. H3, Monmouth Junction, NJ 08852, USA. Tel.: +1 732 274 0657; fax: +1 866 332 3005.

E-mail address: mct@cz-na.com (M.C. Trachtenberg).

removal was nearly 99%. Wang et al. (2004) had similar findings. All these studies support the merit of using a membrane-based contacting device. Importantly, none of these studies examined desorption of the CO<sub>2</sub>-rich amine. Desorption is the critical step; it is both rate-limiting and energy-intensive.

Absorption and desorption can be combined by use of a single unit, a hollow fiber, contained liquid membrane (HFCLM) permeator (Majumdar et al., 1988). This design consists of two sets of microporous hollow fiber membranes with the feed gas flowing through the bore of one set of hollow fibers, the sweep gas (or liquid, vacuum) flowing through the bore of the other set of hollow fibers, and the aqueous liquid membrane located on the shell side between the two fiber sets. Pressure swing absorption (PSA) or vacuum swing absorption (VSA) is used to effect separation. No extra energy is needed to regenerate the absorbent. The liquid membrane can be easily replenished, thus the HFCLM permeator can maintain its performance over a long period of time. Guha et al. (1989) reported the use of aqueous DEA as liquid membrane in a HFCLM permeator to purify biogas, though no details are available.

Guha et al. (1990) modeled and measured the permeabilities and separation factors through a liquid membrane for a CO<sub>2</sub>-N<sub>2</sub> system over a wide range of CO<sub>2</sub> partial pressures. Their approach used an immobilized liquid membrane (ILM, also referred to as a supported liquid membrane or SLM) and an aqueous solution of diethanolamine (DEA). In this system, DEA was immobilized in the pores of a hydrophobic microporous polypropylene membrane, and helium gas was used as the sweep. This combined CO<sub>2</sub> absorption and desorption into a single unit that required no external energy. CO<sub>2</sub>/N<sub>2</sub> separation factors of 230–516 were reported.

The model developed by Guha et al. is directly applicable to our HFCLM permeator. Following Dankwerts (1979) and Blanc and Demarais (1984) they took the reaction between CO<sub>2</sub> and DEA to be first order in amine; it was considered a one-step carbamate formation. However, recent studies, as reviewed by Versteeg et al. (1996), clearly indicate that, depending on the amine concentration the reaction may change from first to second order. The reaction behavior can be modeled with a zwitterionic intermediate or a two-step carbamate formation reaction (Kim and Yang, 2000; Wang et al., 2004; Ali, 2004).

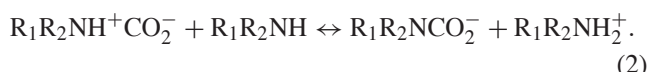
One objective of this work is to implement the two-step carbamate formation mechanism into the facilitated transport model. A second objective is to evaluate the performance of the HFCLM permeator for the separation of CO<sub>2</sub> from a CO<sub>2</sub>-air mixture, using a DEA solution as the liquid membrane, by means of both experimental and numerical methods. Our new results will be compared with those of Guha et al. (1990). The effect of DEA concentrations, liquid membrane thickness and feed CO<sub>2</sub> concentrations on CO<sub>2</sub> transport will be presented. The short-term stability of the permeator will also be demonstrated.

## 2. Theory

The reaction of a secondary amine (R<sub>1</sub>R<sub>2</sub>NH) with dissolved CO<sub>2</sub> is generally described by the zwitterionic mechanism as a two-step sequence. The first step is the formation of an intermediate zwitterion:



In the above reaction, the forward reaction rate constant is  $k_1$ , and the reverse reaction rate constant is  $k_{-1}$ . The zwitterion is deprotonated by the bases present in the solution, forming a carbamate ion and a protonated base



Here the forward reaction rate constant is  $k_{\text{Am}}$  and the reverse reaction rate constant is  $k_{-\text{Am}}$ . Based on the assumption of quasi-steady-state condition for the zwitterionic concentration, the rates of CO<sub>2</sub> reaction with the secondary amine,  $R_{\text{CO}_2}$  and  $R_{\text{R}_1\text{R}_2\text{NH}}$ , can be expressed by

$$R_{\text{CO}_2} = \frac{k_1}{\left(1 + \frac{k_{-1}}{k_{\text{Am}}[\text{R}_1\text{R}_2\text{NH}]}\right)} \left( [\text{CO}_2][\text{R}_1\text{R}_2\text{NH}] - \frac{[\text{R}_1\text{R}_2\text{NCO}_2^-][\text{R}_1\text{R}_2\text{NH}_2^+]}{K_{\text{Eq}}[\text{R}_1\text{R}_2\text{NH}]} \right), \quad (3)$$

$$R_{\text{R}_1\text{R}_2\text{NH}} = 2 \frac{k_1}{\left(1 + \frac{k_{-1}}{k_{\text{Am}}[\text{R}_1\text{R}_2\text{NH}]}\right)} \left( [\text{CO}_2][\text{R}_1\text{R}_2\text{NH}] - \frac{[\text{R}_1\text{R}_2\text{NCO}_2^-][\text{R}_1\text{R}_2\text{NH}_2^+]}{K_{\text{Eq}}[\text{R}_1\text{R}_2\text{NH}]} \right), \quad (4)$$

where the total reaction equilibrium constant,  $K_{\text{Eq}}$ , is defined as

$$K_{\text{Eq}} = \frac{[\text{R}_1\text{R}_2\text{NCO}_2^-][\text{R}_1\text{R}_2\text{NH}_2^+]}{[\text{R}_1\text{R}_2\text{NH}]^2[\text{CO}_2]} = \frac{k_1 k_{\text{Am}}}{k_{-1} k_{-\text{Am}}}. \quad (5)$$

At steady state, the mass balance of CO<sub>2</sub> leads to

$$D_{\text{CO}_2} \frac{d^2[\text{CO}_2]}{dx^2} = R_{\text{CO}_2}, \quad (6)$$

where  $D_{\text{CO}_2}$  is the diffusivity of CO<sub>2</sub>, and  $x$  is the coordinate along the liquid membrane thickness.

Similarly, the mass balance for the free amine in the liquid is

$$D_{\text{R}_1\text{R}_2\text{NH}} \frac{d^2[\text{R}_1\text{R}_2\text{NH}]}{dx^2} = R_{\text{R}_1\text{R}_2\text{NH}}, \quad (7)$$

where  $D_{\text{R}_1\text{R}_2\text{NH}}$  is the diffusivity of amine.

From the electrical neutrality condition, the following equation is obtained:

$$[\text{R}_1\text{R}_2\text{NCO}_2^-] = [\text{R}_1\text{R}_2\text{NH}_2^+]. \quad (8)$$

Assuming equal diffusivity of all amine species leads to

$$C_T = [R_1R_2NH_2^+] + [R_1R_2NH] + [R_1R_2NCO_2^-], \quad (9)$$

where  $C_T$  (in mol/cm<sup>3</sup>) is the total amine concentration and a constant through the liquid membrane.

Eqs. (6) and (7) are to be solved, subject to the following boundary conditions, by assuming no mass transfer resistance in the gas and polymer membrane phases:

$$[CO_2] = H_{CO_2} * P_{f,CO_2}, \quad d[R_1R_2NH]/dx = 0 \quad \text{at } x = 0, \quad (10a)$$

$$[CO_2] = H_{CO_2} * P_{s,CO_2}, \quad d[R_1R_2NH]/dx = 0 \quad \text{at } x = L, \quad (10b)$$

where  $H_{CO_2}$  is Henry's law constant for CO<sub>2</sub> in aqueous amine solution,  $P_{f,CO_2}$  and  $P_{s,CO_2}$  are the feed-side and sweep-side partial pressure of CO<sub>2</sub> across the liquid membrane, and  $L$  is the liquid membrane thickness.

For the case of very low CO<sub>2</sub> partial pressure in the feed or the sweep, mass transfer boundary layer resistance both in the gas phase and membrane phase should be considered. As wetting is also a known phenomenon for microporous membranes and the effect of wetting on the mass transfer is significant, in this work, we also implemented the following boundary conditions for CO<sub>2</sub> with considering the mass transfer resistance in the gas and polymer membrane phases:

$$-D_{CO_2} \frac{d[CO_2]}{dx} = k_{ext}(P_{f,CO_2} - P_{x=0,CO_2}) \quad \text{at } x = 0, \quad (10c)$$

$$-D_{CO_2} \frac{d[CO_2]}{dx} = k_{ext}(P_{x=L,CO_2} - P_{s,CO_2}) \quad \text{at } x = L, \quad (10d)$$

where  $k_{ext}$  is the combined mass transfer coefficient for gas and membrane phase (for simplicity, assume the same value for the feed and sweep sides),  $P$  is the CO<sub>2</sub> partial pressure.

The total flux of CO<sub>2</sub> through the liquid membrane is obtained by

$$N_T^{CO_2} = -D_{CO_2} \left. \frac{d[CO_2]}{dx} \right|_{x=0} = -D_{CO_2} \left. \frac{d[CO_2]}{dx} \right|_{x=L}. \quad (11)$$

The unassisted CO<sub>2</sub> flux through liquid membrane,  $N_{CO_2}$ , is simply

$$N_{CO_2} = -D_{CO_2} \frac{[CO_2]_{x=0} - [CO_2]_{x=L}}{L}. \quad (12)$$

The facilitating factor,  $F$ , is then defined as

$$F = \frac{N_T^{CO_2}}{N_{CO_2}} - 1. \quad (13)$$

The permeance,  $Q$ , is defined as

$$Q = \frac{N}{P_{f,CO_2} - P_{s,CO_2}} \quad (14)$$

and selectivity of the two gases ( $i$  and  $j$ ),  $S$ , as

$$S = \frac{Q_i}{Q_j}. \quad (15)$$

Combining Eqs. (3), (4), (6)–(9), the resulting equations can be nondimensionalized to

$$\frac{d^2C_1}{dy^2} = \left( \frac{\alpha_1}{1 + \alpha_2/C_2} \right) \left( C_1C_2 - \alpha_3 \frac{(1 - C_2)^2}{C_2} \right), \quad (16)$$

$$\frac{d^2C_2}{dy^2} = \left( \frac{\alpha_4}{1 + \alpha_2/C_2} \right) \left( C_1C_2 - \alpha_3 \frac{(1 - C_2)^2}{C_2} \right), \quad (17)$$

where

$$C_1 = \frac{[CO_2]}{H_{CO_2} P_{f,CO_2}}, \quad C_2 = \frac{[R_1R_2NH]}{C_T}, \quad y = \frac{x}{L},$$

$$\alpha_1 = \frac{L^2 k_1 C_T}{D_{CO_2}}, \quad \alpha_2 = \frac{k_{-1}}{k_{Am} C_T},$$

$$\alpha_3 = \frac{1}{4K_{Eq} H_{CO_2} P_{f,CO_2}}, \quad \alpha_4 = \frac{2L^2 k_1 H_{CO_2} P_{f,CO_2}}{D_{R_1R_2NH}}. \quad (18)$$

Boundary conditions (Eq. (10)) are made dimensionless by

$$y = 0, \quad C_1 = 1, \quad \frac{dC_2}{dy} = 0,$$

$$y = 1, \quad C_1 = \frac{P_{s,CO_2}}{P_{f,CO_2}}, \quad \frac{dC_2}{dy} = 0 \quad (19a)$$

or

$$y = 0, \quad \frac{dC_1}{dy} = \left( -\frac{k_{ext}L}{D_{CO_2} H_{CO_2}} \right) (1 - C_1), \quad \frac{dC_2}{dy} = 0,$$

$$y = 1, \quad \frac{dC_1}{dy} = \left( -\frac{k_{ext}L}{D_{CO_2} H_{CO_2}} \right) \left( C_1 - \frac{P_{s,CO_2}}{P_{f,CO_2}} \right),$$

$$\frac{dC_2}{dy} = 0. \quad (19b)$$

Numerical solution of the facilitated transport equations (Eqs. (16), (17) and (19)) is achieved by using the Finite Difference method. Initial guess values were generated by assuming that all reactions were at chemical equilibrium.

### 3. Experimental

Microporous hollow fiber membrane mat, Celgard<sup>®</sup> X30-240, was obtained from Membrana-Charlotte (Charlotte, NC). The outer diameter of the fiber is 300 μm, inner diameter 240 μm, nominal porosity 40% and effective pore size is 0.04 μm. The feed fiber mat and sweep fiber mat are arranged orthogonally in the HFCLM core. The total feed membrane area is about 0.1885 m<sup>2</sup>. The liquid membrane fills the void space between fibers. The thickness of the liquid membrane is controlled by the yarn diameter used to weave the hollow fiber mat. This thickness is taken as the minimum achievable thickness. If a thicker liquid

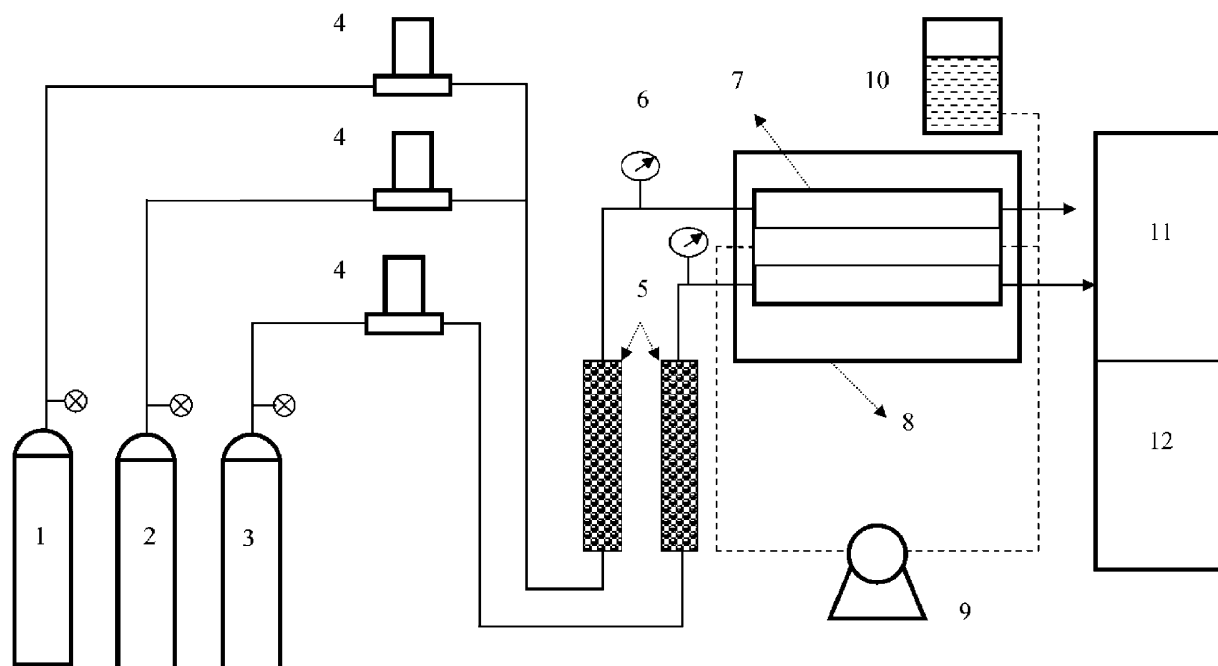


Fig. 1. Diagram of the experimental apparatus. Note: 1—Air; 2—CO<sub>2</sub>; 3—Argon; 4—Mass flow controller; 5—Nafion humidifier; 6—Temperature/Humidity/Pressure meters; 7—HFCLM permeator; 8—Water bath; 9—Liquid circulation pump; 10—Water Reservoir; 11—Mass Spectrometer; 12—Computer.

membrane is needed, additional spacing materials (such as cheesecloth) can be sandwiched between the hollow fiber mats.

Air containing a specific amount of CO<sub>2</sub> (1–20%) was fed to the feed fibers, while ultrahigh purity argon was used as sweep. Both the feed and sweep gases were humidified by passing through a Nafion humidifier. The HFCLM permeator was placed in a temperature-controlled water bath kept constant at 25 °C. The composition of each gas stream was analyzed by an ABB Extrel residual gas analyzing mass spectrometer. The CO<sub>2</sub> concentration in the feed was set by an Environics Mass Flow Controller, while the concentration of CO<sub>2</sub> in the sweep was controlled by adjusting the sweep gas flow rate to achieve a permeate CO<sub>2</sub> concentration at about one tenth that of the feed as determined by mass spectrometer. Fig. 1 shows the diagram of the apparatus.

#### 4. Results and discussion

The liquid membrane thickness was determined experimentally using pure N<sub>2</sub> as a feed and pure water as the liquid membrane. The permeability of N<sub>2</sub> in water is known to have a value of  $1.867E-14$  mol/m<sup>2</sup> s Pa ( $5.58E-9$  (cm<sup>3</sup>(STP) cm)/(cm<sup>2</sup> s cmHg)) (Guha et al., 1989). From this value, we determined that the thickness of the liquid membrane in the HFCLM permeator used in this study is very close to 250 μm. The permeance of CO<sub>2</sub> and the selectivities of CO<sub>2</sub> to N<sub>2</sub> as well as CO<sub>2</sub> to O<sub>2</sub> were measured using pure water as the liquid membrane. The measured CO<sub>2</sub> per-

Table 1  
Observed performance of air–CO<sub>2</sub>–20% DEA solution system

CO <sub>2</sub> % (feed)	CO <sub>2</sub> % (sweep)	CO <sub>2</sub> permeance (mol/m <sup>2</sup> s Pa)	CO <sub>2</sub> /N <sub>2</sub> selectivity	CO <sub>2</sub> /O <sub>2</sub> selectivity
0.86	0.27	5.01E–08	442	270
4.46	1.01	2.77E–08	227	152
9.08	1.60	1.92E–08	153	107
13.83	2.02	1.51E–08	115	83
18.64	2.34	1.25E–08	90	68

meance is  $6.22E-9$  mol/m<sup>2</sup> s Pa. The selectivity of CO<sub>2</sub>/N<sub>2</sub> is 39.0, and 20.0 for CO<sub>2</sub>/O<sub>2</sub>. These data are in excellent agreement with results from Majumdar et al. (1988), who observed that the separation factor for a CO<sub>2</sub>/N<sub>2</sub> system as 37.7.

Table 1 shows the measured CO<sub>2</sub> permeance, CO<sub>2</sub>/N<sub>2</sub> and CO<sub>2</sub>/O<sub>2</sub> selectivity of air–CO<sub>2</sub> mixture through 20% DEA aqueous liquid membrane in the HFCLM permeator. The CO<sub>2</sub> concentration in the feed gas mixtures varied from 1% to 20%. Because of the complex flow pattern of our permeator the listed values of feed-side CO<sub>2</sub> concentrations were taken as the average of the feed and the retentate concentration, and the sweep-side CO<sub>2</sub> concentrations were taken as the average of the sweep and the permeate concentration. The total pressure of the feed gas mixture was kept slightly above atmospheric. The facilitation factors are also shown in Table 1. As expected, the CO<sub>2</sub> permeance decreased with increasing feed CO<sub>2</sub> concentration; this is also the case for

Table 2  
Physicochemical parameters used

Parameter	Value	Source
Solubility ( $H_{1w}$ )	$4.45E-7 \text{ mol/cm}^3 \text{ cmHg}$	Guha et al. (1990)
Diffusivity ( $D_{CO_2w}$ )	$1.92E-5 \text{ cm}^2/\text{s}$	Guha et al. (1990)
Diffusivity ( $D_{R_1R_2NH}$ )	$3.83E-6 \text{ cm}^2/\text{s}$	Guha et al. (1990)
Reaction constant ( $k_1$ )	$3.17E6 \text{ cm}^3/\text{mol s}$	Yamaguchi et al. (1995)
Equilibrium constant ( $K_{Eq}$ )	$1.43E6 \text{ cm}^3/\text{mol}$	Yamaguchi et al. (1995)
Reaction constant ratio ( $k_{-1}/k_{Am}$ )	$4.58E-3 \text{ mol/cm}^3$	Yamaguchi et al. (1995)

the facilitation factors. The selectivity of  $CO_2/N_2$  is six-fold that for the pure water system. The  $CO_2/O_2$  selectivity is about half of the  $CO_2/N_2$  selectivity. The amine-based facilitated transport accounts for the major contribution of this increase, while the rest comes from the decreased solubility of non-reactive gases in the amine solution.

We compared the experimental results with the data derived from the numerical simulation shown above. The physicochemical parameters (diffusivity and solubility) used in the simulation were taken from Guha et al. (1990). The estimated diffusivity and solubility values used in the simulations are provided in Table 2. The kinetic parameters of the  $CO_2$ -amine reaction in aqueous solution are taken from Yamaguchi et al. (1995). The values of these parameters are also listed in Table 2. The diffusivity of gases in DEA solution was correlated with the concentration of DEA solution ( $C_T$ ,  $\text{mol/cm}^3$ ) by the following equation:

$$\frac{D_{iAm}}{D_{iw}} = \left( \frac{D_{Am}}{D_w} \right) \Big|_{N_2O} = 1.0 - 1.1352 \times 10^2 C_T. \quad (20)$$

The solubility was correlated by the following equation from experimental results derived from Sada et al. (1977).

$$\ln \left( \frac{H_{iAm}}{H_{iw}} \right) = - (1.0406 \times 10^{-4} + 6.8433 \times C_T + 1.33633 \times 10^4 C_T^2 - 1.1549 \times 10^6 C_T^3). \quad (21)$$

These formulas, Eqs. (20) and (21), were adopted from Blanc and Demarais (1984) and Guha et al. (1990) and they correct errors found in the formulas printed in these articles.

Typical concentration profiles for all the species across the liquid membrane are shown in Fig. 2 for two different  $CO_2$  partial pressure conditions. The data show that at lower feed  $CO_2$  partial pressure the  $CO_2$  gradients are much steeper near the membrane-liquid boundaries than that at higher feed  $CO_2$  partial pressure. Thus, a higher facilitation factor is found at the lower  $CO_2$  feed partial pressure. At the higher  $CO_2$  feed concentration, the facilitation factor becomes very small, meaning no benefit is derived from the facilitator.

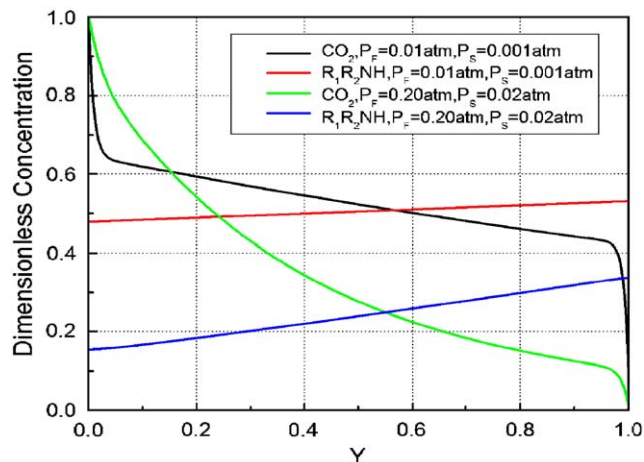


Fig. 2. Simulated dimensionless concentration profile of  $CO_2$  and amine species at two different  $CO_2$  feed concentrations. Other parameters: DEA = 20%,  $L = 200 \mu\text{m}$ , Temperature = 298.15 K.

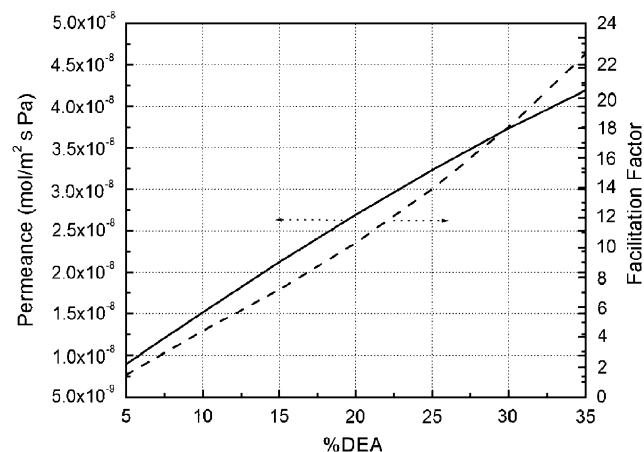


Fig. 3. Effect of DEA concentration on  $CO_2$  permeance and facilitation factor from simulation. Other parameters:  $P_{CO_2}$  (feed) = 0.10 atm,  $P_{CO_2}$  (sweep) = 0.01 atm,  $L = 200 \mu\text{m}$ , Temperature = 298.15 K.

Fig. 3 illustrates the effect of amine concentration on  $CO_2$  transport. As the amine concentration decreases, less of the chemical facilitator is available for the reactive transport process. This results in lower permeance, as anticipated. However, the gas diffusivity and solubility become higher at lower amine concentration. As shown in Fig. 3, as DEA concentration increases, both permeance and facilitation factor increase, but the increase rate at higher amine concentration is less than that at lower amine concentration.

The membrane thickness also has a considerable affect on facilitated transport. The thicker the liquid membrane, the longer the residence time, thus the greater the facilitation (Majumdar et al., 1988). If the residence time is sufficiently large, chemical equilibrium can be achieved. This gives the highest facilitation factor and the highest selectivity. The adverse effect of a thicker membrane is to reduce flux, as the

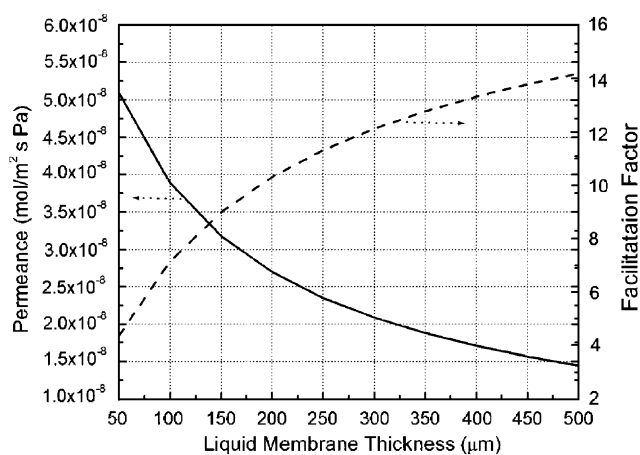


Fig. 4. Effect of liquid membrane thickness on  $\text{CO}_2$  permeance and facilitation factor from simulation. Other parameters:  $P_{\text{CO}_2}$  (feed) = 0.10 atm,  $P_{\text{CO}_2}$  (sweep) = 0.01 atm,  $L = 200 \mu\text{m}$ , Temperature = 298.15 K.

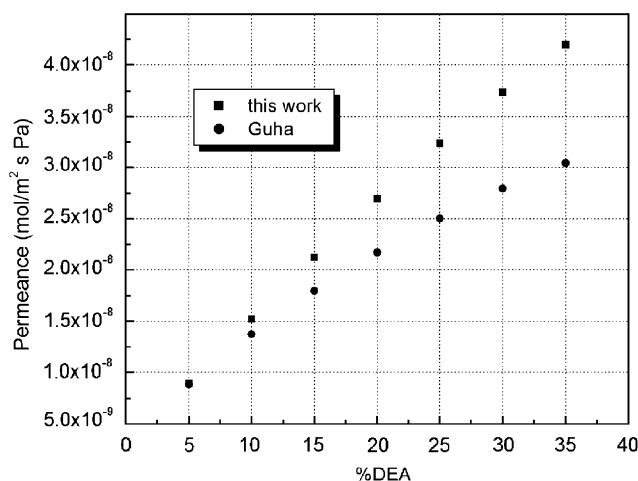


Fig. 6. Comparison between this work and that of Guha et al. (1990). Other parameters:  $P_{\text{CO}_2}$  (feed) = 0.10 atm,  $P_{\text{CO}_2}$  (sweep) = 0.01 atm,  $L = 200 \mu\text{m}$ , Temperature = 298.15 K.

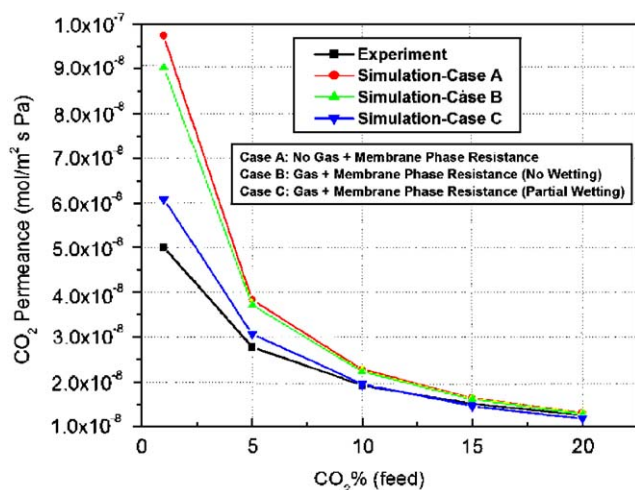


Fig. 5. A comparison of  $\text{CO}_2$  permeance values derived from experimental and simulation data.  $P_{\text{CO}_2}$  (feed) = 0.0086–0.188 atm,  $P_{\text{CO}_2}$  (sweep) = 0.0038–0.0424 atm, DEA = 20%,  $L = 200 \mu\text{m}$ , Temperature = 298.15 K.

flux is inversely proportional to the membrane thickness. The effect of membrane thickness on permeance as well as facilitation factor is shown in Fig. 4. These exhibit the same trend as is seen for flux. A thinner liquid membrane gives higher permeance. The permeance approaches an asymptote as the membrane thickness increases. The facilitation factor also approaches an asymptote, the chemical equilibrium limit.

Fig. 5 compares the measured and simulated permeance for the applications of low  $\text{CO}_2$  partial pressure (< 15 kPa). Three different situations were considered. For Case A, there is no external mass transfer resistance in the gas or the membrane phase, for Case B, mass transfer resistance was estimated and included in the simulation, and for Case C, partial wetting in the membrane pores was assumed. The simulation

results are in very good agreement with the measured values at higher feed  $\text{CO}_2$  partial pressure. The principal discrepancy is seen at lower feed  $\text{CO}_2$  partial pressures under conditions of no external mass transfer resistance (Case A). The boundary layer mass transfer resistances in the gas phase and polymer membrane phase at lower  $\text{CO}_2$  partial pressure contribute to this discrepancy. As shown in Case B, which incorporated external mass transfer resistance, the predicted performance at lower feed  $\text{CO}_2$  partial pressure improved only about 10%. In view of the work of Rangwala (1996), who specifically demonstrated DEA wetting of polypropylene micropores, there is strong reason to suspect that the DEA is wetting our polypropylene membrane. He reported wetting resulting in 0.9% liquid filled pores. If we assume that 1 of 100  $\mu\text{m}$  long pore was wetted, as shown in Case C, the simulation becomes much closer to the experimental value. A detailed analysis of the effect of gas phase and membrane phase (with possible partial wetting) is given in Appendix A.

As discussed above, a two-step carbamate formation mechanism was used in this work instead of one-step carbamate formation used previously. A detailed examination of the transport governing equations reveals that the only difference between these two mechanisms is the factor,  $1/(1+k_{-1}/(k_{\text{Am}}[R_1R_2NH]))$ . As shown in Table 2, the value of  $k_{-1}/k_{\text{Am}}$  is small, on the order of  $4.58\text{E} - 3 \text{ mol/cm}^3$ . The molar concentration of 20% DEA solution at 25 °C is about  $1.94\text{E} - 3 \text{ mol/cm}^3$ , thus, the value of this factor is about 0.2976. At 30% DEA it will be 0.389 and 0.175 at 10% DEA. Thus, the difference between these two mechanisms will vary, depending on the concentration of DEA solution. The  $\text{CO}_2$  permeances calculated at low  $\text{CO}_2$  partial pressures using these two mechanisms are compared in Fig. 6. These results were calculated on the basis of the parameter values in Table 2. The effect of these differences

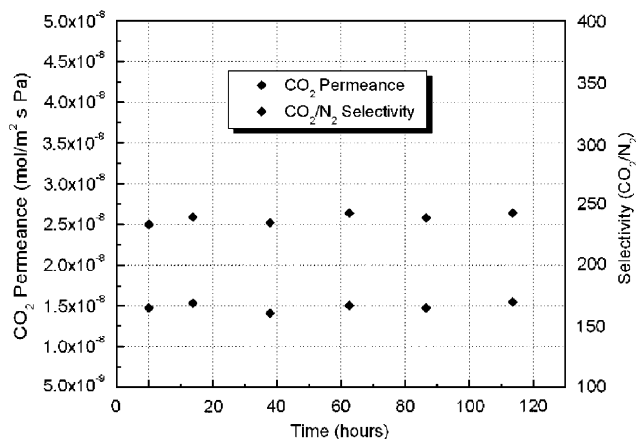


Fig. 7. Short-term stability of HFCLM permeator.  $P_{\text{CO}_2}$  (feed)=0.01 atm,  $P_{\text{CO}_2}$  (sweep) = 0.001 atm, Temperature = 298.15 K.

becomes obvious and progressively greater at DEA concentrations in excess of 5%. At high  $\text{CO}_2$  partial pressures, such as those used in the work of Guha et al., the two-step mechanism will still yield a permeance that is slightly higher than the one-step mechanism, as confirmed by the simulations. As noted in Guha et al. (1990), “Though the present model predicted the separation factors quite well, the permeability values of  $\text{CO}_2$  were always overpredicted to a great extent.” They attributed this discrepancy to the uncertainties of other parameters, e.g., diffusivity of amine, rate constants, etc. As the same set of parameters were used in this work, save the reaction rate constants, a similar discrepancy should be expected for the two-step model. However, since the two-step model gives good prediction for our low  $\text{CO}_2$  partial pressure applications, the dependence of solubility on the pressure should be examined.

The short-term stability of the HFCLM–FTMC was also examined. Fig. 7 illustrates both the  $\text{CO}_2$  permeance and the  $\text{CO}_2/\text{N}_2$  selectivity over a continuous test lasting 5 days. As shown in the figure, the  $\text{CO}_2$  permeance is virtually constant over this period, so too is the  $\text{CO}_2/\text{N}_2$  selectivity. Given such good results, we are confident of longer-term stability of this design.

## 5. Conclusions

$\text{CO}_2$ -facilitated transport across a thin secondary amine (DEA) solution was evaluated through experiment and simulation. A two-step carbamate formation mechanism was incorporated in the simulation, instead of the one-step mechanism used by previous investigators. A comparison of these two mechanisms was provided. The effects of feed  $\text{CO}_2$  partial pressure, liquid membrane thickness and concentration of amine solutions on  $\text{CO}_2$  permeance and facilitation factors were also investigated. Our predictions are in good agreement with the experimental data for feed  $\text{CO}_2$  concentrations of industrial importance, and significant improve-

ment in the accuracy of prediction was obtained by including mass transfer resistances in the gas and membrane phase, with particular emphasis on wetting at lower  $\text{CO}_2$  partial pressure.

## Acknowledgements

We gratefully acknowledge support from NASA Grant no. NAG9-1383 and the DOE, Grant no. DE-FG02-02ER83380. Special thanks to Dr. Jerry Meldon for excellent discussions and suggestions.

## Appendix A. Analysis of gas and membrane phase mass transfer coefficients

The mass transfer coefficients in the gas phase and membrane phase can be obtained from available correlations. For gas flow in the hollow fiber bore, the follow correlation can be used to predict the gas-phase mass transfer coefficient,  $k_g$

$$Sh = \frac{k_g d}{D} = 1.62 * Gr^{1/3}, \quad (\text{A.1})$$

where  $d$  is diameter of the fiber,  $D$  is  $\text{CO}_2$  diffusivity in air,  $Gr$  is Gratzke number ( $Gr = v * d^2/L/D$ ). Eq. (A.1) is valid only for  $Gr > 20$ . For the permeator used in these experiments,  $Gr$  is about 0.0125, which means Eq. (A.1) is not useful for the current system. Other correlations can also be used. Rangwala (1996) provided the following correlation for estimating  $k_g$  in their air– $\text{CO}_2$ –water system

$$k_g = 0.007839 * (P_T/P_{BM}) * (v_g)^{0.83}, \quad (\text{A.2})$$

where  $P_T$  and  $P_{BM}$  are the total pressure and the long-mean partial pressure of air.

Based on current permeator design and experimental parameters,  $k_g$  at feed side is estimated to be 0.01 m/s.  $k_g$  at sweep side is about the same.

The resistance to mass transfer within the membrane comes from both the presence of a stagnant gas within the membrane pore and the membrane structure. Due to the very fine pore in the membrane wall, we expect that Knudson diffusion is significant. The effective diffusivity ( $D_{gm,eff}$ ) can then be written as

$$\frac{1}{D_{gm,eff}} = \frac{1}{D_{g,b}} + \frac{1}{D_K} \quad (\text{A.3})$$

and  $D_K$  is calculated from Eq. (A.4):

$$D_K = \frac{1}{3} * d_p * \sqrt{\frac{8RT}{\pi M}}, \quad (\text{A.4})$$

where  $d_p$  is the pore diameter,  $R$  the gas constant,  $T$  the temperature,  $M$  the molecular weight. For  $\text{CO}_2$  in Celgard X-30 PP hollow fibers,  $D_K = 3.85 \times 10^{-6} \text{ m}^2/\text{s}$ , whereas  $D_{g,b} = 1.70 \times 10^{-5} \text{ m}^2/\text{s}$ .

The effective membrane mass transfer coefficient can be estimated from Eq. (A.5):

$$k_m = \frac{D_{gm,eff} \varepsilon}{\tau t} \quad (\text{A.5})$$

and the  $k_m$  value for feed side fiber is 0.00785 m/s, and for sweep fiber the value is 0.007725 m/s.

The values obtained above are valid only for the non-wetting case, when the pores of the hollow fiber membrane are completely occupied by gas. However, Rangwala (1996) observed wetting in his air–CO<sub>2</sub>–DEA polypropylene hollow fiber contactor system. This is the same type of hollow fiber membrane was used in our system. The membrane mass transfer coefficient ( $k_m$ ) equals 0.00065 m/s, about 10 times smaller than the calculated value from Eq. (A.5). He attributed this to the partial wetting of the membrane that resulted from the surface modification by DEA and other contaminants, that, in turn, allows some penetration of the liquid solution into the pores. He estimated that the average fractional depth of liquid penetration is less than 1%.

In the simulations shown as Case C in Fig. 5, the external (gas + membrane with partial wetting) mass transfer coefficient ( $k_{ext}$ ) was set at 0.001 m/s.

## References

- Ali, S.H., 2004. Kinetic study of the reaction of diethanolamine with carbon dioxide in aqueous and mixed solvent systems—application to acid gas cleaning. *Separation and Purification Technology* 38, 281–296.
- Blanc, C., Demarais, G., 1984. The reaction rate of CO<sub>2</sub> with diethanolamine. *International Chemical Engineering* 24, 43–52.
- Dankwerts, P.V., 1979. The reaction of CO<sub>2</sub> with ethanolamines. *Chemical Engineering Science* 34, 443–446.
- Falk-Pedersen, O., Dannstrom, H., Witzko, R., Bier, C., 1999. Natural gas sweetening using membrane gas/liquid contactor. The 49th Laurance Reid Gas Conditioning Conference, pp. 405–417.
- Guha, A.K., Majumdar, S., Lee, Y.T., Sirkar, K.K., 1989. HFCLM purification of biogas: aqueous DEA solution as liquid membrane. A.I.Ch.E. National Meeting, Houston, TX.
- Guha, A.K., Majumdar, S., Sirkar, K.K., 1990. Facilitated transport of CO<sub>2</sub> through an immobilized liquid membrane of aqueous diethanolamine. *Industrial Engineering Chemical Research* 29, 2093–2100.
- Kim, Y.S., Yang, S.M., 2000. Absorption of carbon dioxide through hollow fiber membranes using various aqueous absorbents. *Separation and Purification Technology* 21, 101–109.
- Majumdar, S., Guha, A.K., Sirkar, K.K., 1988. A new liquid membrane technique for gas separation. *A.I.Ch.E. Journal* 34, 1135–1145.
- Mavroudi, M., Kaldis, S.P., Sakellariopoulos, G.P., 2003. Reduction of CO<sub>2</sub> emission by a membrane contacting process. *Fuel* 82, 253–259.
- Rangwala, H.A., 1996. Absorption of carbon dioxide into aqueous solutions using hollow fiber membrane contactors. *Journal of Membrane Science* 112, 229–240.
- Sada, E., Kurmazawa, H., Butt, M., 1977. Solubilities of gases in aqueous solutions of amine. *Journal of Chemical Engineering Data* 22, 277–278.
- Versteeg, G.F., Dijk, L.A.J., Swaaij, P.M., 1996. On the kinetics between CO<sub>2</sub> and alkanolamines both in aqueous and non-aqueous solutions: an overview. *Chemical Engineering Communication*, 113–158.
- Wang, R., Li, D.F., Liang, D.T., 2004. Modeling of CO<sub>2</sub> capture by three typical amine solutions in hollow fiber membrane contactors. *Chemical Engineering and Processing* 43, 849–856.
- Yamaguchi, T., Boetje, L.M., Koval, C.A., Noble, R.D., Bowman, C.N., 1995. Transport properties of carbon dioxide through amine functionalized carrier membranes. *Industrial Engineering Chemical Research* 34, 4071–4077.